JOURNAL OF VIROLOGY, May 2006, p. 4264–4275 Vol. 80, No. 9
0022-538X/06/$08.00+0 doi:10.1128/JVI.80.9.4264–4275.2006

Reconstitution of Herpes Simplex Virus Microtubule-Dependent Trafficking In Vitro†

Grace E. Lee,[1] John W. Murray,[2] Allan W. Wolkoff,[2] and Duncan W. Wilson[1]*

Department of Developmental and Molecular Biology,[1] and Marion Bessin Liver Research Center and Department of Anatomy and Structural Biology,[2] Albert Einstein College of Medicine, Bronx, New York 10461

Received 27 September 2005/Accepted 31 January 2006

Microtubule-mediated anterograde transport of herpes simplex virus (HSV) from the neuronal cell body to the axon terminal is crucial for the spread and transmission of the virus. It is therefore of central importance to identify the cellular and viral factors responsible for this trafficking event. In previous studies, we isolated HSV-containing cytoplasmic organelles from infected cells and showed that they represent the first and only destination for HSV capsids after they emerge from the nucleus. In the present study, we tested whether these cytoplasmic compartments were capable of microtubule-dependent traffic. Organelles containing green fluorescent protein-labeled HSV capsids were isolated and found to be able to bind rhodamine-labeled microtubules polymerized in vitro. Following the addition of ATP, the HSV-associated organelles trafficked along the microtubules, as visualized by time lapse microscopy in an imaging microchamber. The velocity and processivity of trafficking resembled those seen for neurotropic herpesvirus traffic in living axons. The use of motor-specific inhibitors indicated that traffic was predominantly kinesin mediated, consistent with the reconstitution of anterograde traffic. Immunocytochemical studies revealed that the majority of HSV-containing organelles attached to the microtubules contained the *trans*-Golgi network marker TGN46. This simple, minimal reconstitution of microtubule-mediated anterograde traffic should facilitate and complement molecular analysis of HSV egress in vivo.

The herpes simplex virus (HSV) particle consists of a ~152-kb DNA genome contained within an icosahedral capsid. A complex layer of proteins termed tegument lies between the capsid and the viral envelope, a lipid bilayer obtained from a host cell cytoplasmic organelle that contains multiple membrane proteins, most of which are glycosylated. During infection, the envelope and host cell plasma membranes fuse, the capsid and associated tegument polypeptides enter the cytoplasm, and the capsid travels from the periphery of the cell to the vicinity of the nucleus via retrograde microtubular traffic by utilizing dynein motors (6, 21, 22, 46, 60, 62, 70). The DNA genome is replicated and transcribed in the nucleoplasm, and progeny capsids are assembled.

Following the packaging of progeny procapsids with newly replicated viral genomes, the mature nucleocapsids undergo a round of envelopment and deenvelopment at the nuclear membranes (13, 57) and enter the cytoplasm. They then acquire their final, mature envelope by budding into a cytoplasmic organelle (7, 9, 26, 30, 37, 48, 53, 57, 63, 67). In sensory neurons, capsids and/or enveloped particles utilize microtubule-mediated anterograde traffic to travel to the nerve terminal for subsequent release from the cell. A number of elegant ultrastructural and live-cell imaging studies using both herpes simplex virus and pseudorabies virus (PRV) have begun to define the kinetics and saltatory nature of this anterograde flow and the structural composition of the trafficking particles (4, 17, 32, 45, 49, 50, 58, 59, 69).

In previous studies, we utilized subcellular fractionation techniques to isolate HSV-associated organelles from the cytoplasm of infected cells (30). We demonstrated that these organelles were distinct from the *cis*, medial, and *trans* cisternae of the Golgi apparatus but that they did cofractionate with the *trans*-Golgi network (TGN) marker TGN46 and with endosomes (30). Utilizing a synchronous HSV assembly assay (14), we further showed that this organellar fraction is the first and only destination for enveloping HSV capsids after they emerge from the nucleus (30).

We reasoned that these HSV-associated organelles might be capable of anterograde microtubular traffic in vitro. If so, such a system would facilitate a biochemical dissection of the cellular and viral factors required for HSV egress in neurons and complement the elegant live-cell imaging studies described previously (17, 45, 58, 59). Here, we report the ATP-dependent in vitro traffic of these HSV-associated organelles upon purified microtubules in an optical imaging chamber. The velocity and processivity of traffic is similar to that seen for HSV and PRV in living axons. Also similar to the in vivo situation, traffic is predominantly anterograde [as it is largely blocked in the presence of the kinesin inhibitor adenosine 5′-(β,γ-imido)triphosphate (AMP-PNP)]. Finally, we demonstrate that the majority of HSV-containing structures that become microtubule bound colocalize with the TGN marker TGN46. This is consistent with accumulating evidence that the TGN is the principal site of HSV envelopment during egress (48, 63).

MATERIALS AND METHODS

Cells and viruses. Human hepatoma (HuH7) cells were maintained in RPMI medium supplemented with 1% penicillin-streptomycin (Gibco Laboratories) and 10% fetal calf serum. Vero cells were grown in Dulbecco's modified Eagle's medium–1% penicillin-streptomycin supplemented with 10% newborn calf serum (GIBCO Laboratories). A green fluorescent protein (GFP)-VP26-expressing HSV

* Corresponding author. Mailing address: Department of Developmental and Molecular Biology, Albert Einstein College of Medicine, 1300 Morris Park Avenue, Bronx, NY 10461. Phone: (718) 430-2305. Fax: (718) 430-8567. E-mail: wilson@aecom.yu.edu.

† Supplemental material for this article may be found at http://jvi.asm.org/.

strain, K26GFP (18), was grown, and the titers of the virus were determined by plaque assay on Vero cell monolayers as previously described (14).

Isolation of organelle-associated HSV. HuH7 or Vero cells were infected at a multiplicity of infection of 50 with HSV strain K26GFP for 1 h at 37°C and then overlaid with fresh prewarmed medium. At 12 h postinfection, the cells were washed twice in ice-cold MEPS buffer {5 mM $MgSO_4$, 5 mM EGTA, 0.25 M sucrose, 35 mM PIPES [piperazine-*N*,*N*′-bis(2-ethanesulfonic acid)], pH 7.1} (52), collected by scraping, and resuspended in MEPS buffer supplemented with 2 mM phenylmethylsulfonyl fluoride, 2% (vol/vol) protease inhibitor cocktail (Sigma), and 4 mM dithiothreitol (DTT). To isolate postnuclear supernatants (PNSs), the cells were broken by passage through a 25-gauge needle and centrifuged at 2,000 × *g* at 4°C for 10 min to pellet nuclei (30). The resulting PNS was adjusted to 1.4 M sucrose using 2.5 M sucrose in MEPS buffer. This was loaded at the bottom of a sucrose step gradient consisting of 1.4 M, 1.2 M, and 0.25 M sucrose in MEPS and centrifuged in a TLS55 rotor (Beckman) for 165 min at 101,000 × *g*. After centrifugation, the cloudy interface between the 1.2 M and 0.25 M sucrose layers was collected. Collected material was adjusted to 4 mM DTT, 2 mM phenylmethylsulfonyl fluoride, and 2% (vol/vol) protease inhibitor cocktail. Aliquots were frozen in liquid nitrogen and stored at −70°C.

Preparation of fluorescent microtubules. Unlabeled and rhodamine-labeled tubulins (Cytoskeleton) were mixed at a ratio of 10:1 (total concentration of 6.5 μg/μl) in BRB80/G buffer (80 mM PIPES, pH 6.8, 1 mM EGTA, 1 mM $MgCl_2$, 1 mM GTP, 3% glycerol) (34). The mixture was polymerized at 37°C for 15 min and then stabilized by adding prewarmed BRB80/GT buffer (BRB80/G buffer plus 20 μM taxol). Microtubules were pelleted to remove nonpolymerized tubulin by centrifugation through 30% glycerol made in BRB80/GT buffer at 15 lb/in^2 at room temperature in a Beckman Airfuge. The pelleted microtubules were resuspended in BRB80/GT buffer and stored at room temperature in the dark. For chamber assays, microtubules were diluted in PMEE buffer (35 mM PIPES, 5 mM $MgSO_4$, 1 mM EGTA, 0.5 mM EDTA, pH 7.4) supplemented with 20 μM taxol at various concentrations, and the final concentration of the microtubules was determined by examining their density using fluorescence microscopy.

Construction of an optical microchamber. An optical chamber was prepared as previously described (51, 52). The chamber was constructed by placing a piece of cut glass slide (~22 by 8 mm) on top of two pieces of double-stick tape (Scotch; 3M) that were in turn placed onto a large coverslip (Corning). This creates a chamber that holds a total volume of 3 to 5 μl. To enhance microtubule binding and to avoid nonspecific binding of organelles, the coverslip was coated with 20 μg/ml DEAE-dextran (Pharmacia) prior to chamber assembly.

Motility assay. Motility assays were performed similarly to those previously described (52). Microtubules diluted in PMEE buffer plus 20 μM taxol (as described above) were introduced into the DEAE-dextran-coated chamber. After 3 min of incubation, the chamber was washed with blocking buffer (assay buffer [PMEE buffer, 20 μM taxol, 2 mg/ml bovine serum albumin, 4 mM DTT, 2 mg/ml ascorbic acid] plus 5 mg/ml casein). The gradient-purified HSV-associated organelle suspension was thawed, diluted into assay buffer, if necessary, and perfused into the chamber. After 5 to 10 min of incubation at room temperature, the chamber was washed with assay buffer and placed in a box with a cover to minimize dehydration of the chamber. Motility was initiated with the addition of 500 μM ATP diluted in assay buffer supplemented with or without an ATP-regenerating system (0.16 mg/ml creatine kinase, 8 mM phosphocreatine), and imaging was performed in a microscope station maintained at 37°C with the use of a thermal chamber. During motor inhibitor studies, 1 mM AMP-PNP or 5 M Na_3VO_4 in ATP-containing assay buffer was introduced into the chamber during imaging.

Microchamber immunofluorescence and antibodies. Microchamber immunofluorescence was performed as previously described (51). A concentrated HSV-associated organelle suspension (~4 μl) was incubated in the DEAE-dextran-coated microchambers for 10 min and washed with blocking buffer. The organelle sample was sequentially incubated with a selected primary antibody and a secondary antibody (diluted in blocking buffer) for 5 min each and washed with assay buffer in between incubations. Antibodies were used at concentrations of 10 to 100 μg/ml to allow for short incubations. A drop of glycerol was added at each open edge of the chamber to avoid dehydration before imaging was performed. The following primary antibodies were used: mouse monoclonal anti-Rab4 and anti-Rab5 (Transduction Laboratories), rabbit polyclonal anti-Rab7 (Santa Cruz Biotechnology), and affinity-purified sheep anti-TGN46 antiserum (Serotec). The following secondary antibodies were used: Cy5-conjugated goat anti-mouse immunoglobulin G (IgG) (Jackson Immuno Research), Cy5-conjugated donkey anti-rabbit and anti-sheep IgG (Jackson Immuno Research), Alexa Fluor 568-conjugated goat anti-mouse and anti-rabbit IgG (Molecular Probes), and Alexa Fluor 594 donkey anti-sheep IgG (Molecular Probes).

Light microscopy. All imaging was performed at the Analytical Imaging Facility of the Albert Einstein College of Medicine. Time lapse movies were taken using a cooled charged-coupled-device camera mounted on an Olympus IX81 inverted microscope with a ×60, 1.4-numerical-aperture Plan Apo objective. It also contained automatic excitation and emission filter wheels connected to a Sensicam QE cooled charged-coupled-device camera run by IP Lab Spectrum 3.6.1 software on a personal computer. Sequential imaging showing microtubules and then virus and then microtubules again to initiate the subsequent frame was performed. Time between the initiation of one frame and the initiation of the next frame varied between 4.48 and 4.56 s.

Analysis of images. All images were saved as TIF files and opened using ImageJ 1.31 software to merge red-green-blue (RGB) images. The percentage of motility or colocalization was determined by counting fluorescent particles manually with the help of the Crosshair tool in ImageJ. Velocities of motile particles were obtained by calculating the duration of movement from its timing file and measuring the pixel length of its moving route with the use of the Freehand line selection tool in ImageJ. Since images were collected at multiples of a constant interval (approximately 4.5 s), the time, *t*, during which a particle moves a run length, *l*, is a multiple, *m*, of the sampling interval, *i* (that is, $t = mi$). Velocity, *v*, was calculated as follows: v = (run length)/time; hence, $v = l/mi$. In a plot of velocity versus run length, the slope is v/l or $(l/mi)/l$ or $1/mi$. Thus, the data will lie along discrete lines with slopes inversely proportional to each multiple *m* of the sampling interval *i*.

Electron microscopy. After HSV-containing organelles were attached to microtubules as described above, the microchamber was fixed in 2.5% glutaraldehyde in PMEE buffer at room temperature for 15 min. The microchamber was then washed with PMEE buffer, postfixed in 1% osmium tetroxide in PMEE buffer followed by 1% uranyl acetate, dehydrated through a graded series of ethanols, and embedded in LX112 resin (LADD Research Industries, Burlington, Vt.). Ultrathin sections were cut on a Reichert Ultracut E, stained with uranyl acetate followed by lead citrate, and viewed on a Jeol 1200EX transmission electron microscope at 80 kV.

RESULTS

Cytoplasmic HSV binds to microtubules in vitro. To study HSV trafficking by time lapse fluorescence microscopy, we made use of HSV strain K26GFP (18), in which green fluorescent protein is fused to the capsid subunit VP26. After preparation of a PNS from K26GFP-infected cells, we used our previously established conditions of sucrose gradient centrifugation (30) to prepare cytoplasmic organelles containing mature and enveloping HSV particles. We have previously demonstrated that HSV capsids associate with this organellar fraction immediately after leaving the nucleus and therefore that these organelles are the ones responsible for HSV envelopment and exocytosis (30). We would therefore expect these organelles to be capable of microtubule binding and trafficking.

To examine the interaction of these HSV-associated organelles with microtubules, we used an optical microchamber containing prebound rhodamine-labeled microtubules exactly as previously described (52). Gradient-purified HSV-containing organelles were flowed into the chamber and allowed to attach to the microtubules. Unbound organelles were subsequently removed by washing. Fluorescent microscopy images were taken before and after the washing step in order to measure the efficiency of binding of HSV K26GFP-containing organelles to the microtubules. We observed that approximately 62% of the fluorescent particles added to the chamber became stably bound to the microtubules (data not shown). Figure 1A shows two representative microscopic fields of rhodamine-labeled microtubules and bound organelles containing GFP-labeled HSV capsids. Ultrastructural examination of similar samples revealed that these microtubule-bound structures included both partially or fully enveloped HSV capsids and capsids attached to the surface of organelles (Fig. 1B), structures that we observed in our previous studies (30).

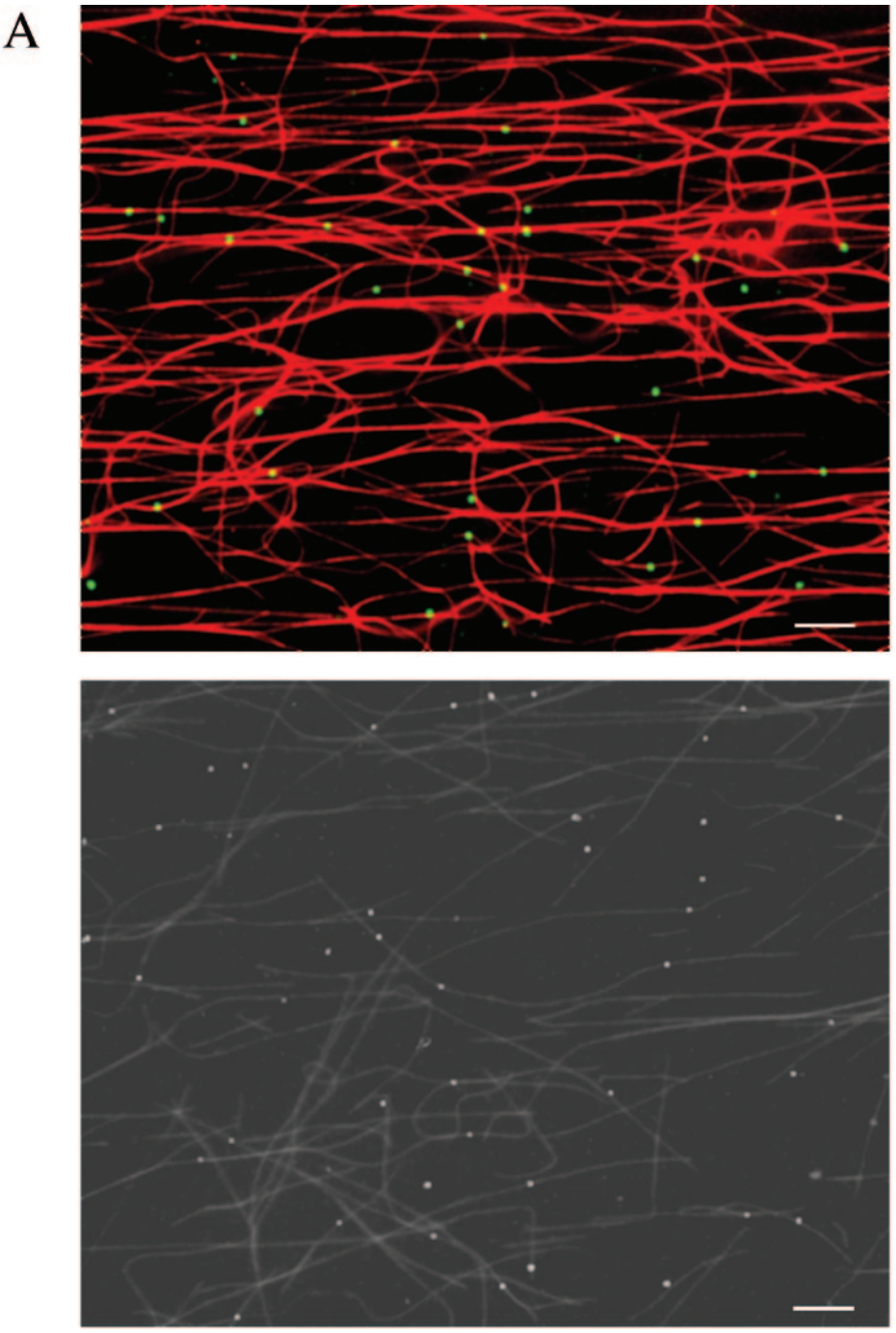

FIG. 1. Membrane-associated cytoplasmic HSV capsids bind to microtubules in vitro. (A) Bouyant organelles were isolated from the cytoplasm of HSV K26GFP-infected cells. They then flowed into an imaging chamber, which contained prebound rhodamine-labeled microtubules. After an incubation of 5 to 10 min, unbound material was washed away, and the chamber was imaged using fluorescence microscopy. The upper panel shows microtubules in red and bound HSV-containing organelles in green. The lower panel is another representative field shown in black and white. Scale bar, 10 μm. (B) HSV was bound to microtubules as in A, and the chamber was then fixed in glutaraldehyde and prepared for transmission electron microscopy as described in Materials and Methods. This representative image appears to show HSV capsids partially or completely enclosed by an organelle (arrowhead) or adjacent to an organelle (black arrow) and in both cases attached to a microtubule (white arrow). Scale bar, 100 nM.

Cytoplasmic HSV traffics along microtubules in an ATP-dependent manner. Gradient-purified cytoplasmic HSV-containing organelles were bound to microtubules as described above, and ATP was then perfused into the chamber. Using time lapse video microscopy, sequential images were then captured every ~4.5 s for approximately 131 s. The green fluorescent particles were observed to demonstrate microtubule-based translocation. Two sets of representative time lapse

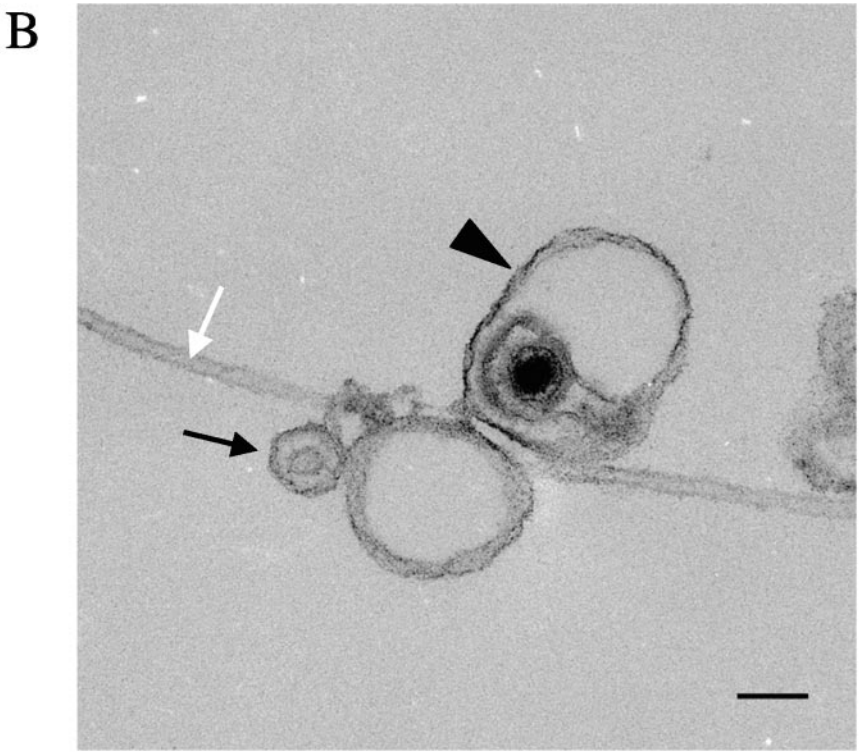

FIG. 1—*Continued.*

images are shown in Fig. 2A and B, and a time lapse movie is included in the supplemental material. The efficiency of motility (defined as the percentage of the total bound fluorescent particles that exhibited motion) was 18.1% (based on a count of 1,595 individual particles).

To gain insight into the mechanism of motility, the travel distance and velocity of each run were examined (a run was defined as a period of uninterrupted travel lacking pauses or reversal in direction). These data were determined for 391 individual motile particles and are summarized in Fig. 3. The average run length was 11.8 ± 0.9 μm (Fig. 3A), with an average velocity of 0.58 ± 0.02 μm/s (Fig. 3B). About 49% of the runs traveled less than 5 μm (Fig. 3A), and 52% were slower than 0.5 μm/s (Fig. 3B). We also noticed that some motile particles (~7.6% of the total trafficking organelles) switched their direction of motion (Fig. 4). This could imply that both plus- and minus-end-directed motors were active; however, it may also be that those particles were moving along closely bundled microtubules and simply switching to an adjacent antiparallel microtubule.

If this in vitro assay system faithfully reproduces the mechanism of microtubule-dependent HSV exocytosis, motility would be primarily plus-end directed and mediated by kinesins. To test the contribution of plus- and minus-end-directed motors to the observed HSV-containing organelle motility, we examined the effect of specific motor protein inhibitors. AMP-PNP at a concentration of 1 mM is known to inhibit kinesins (64), whereas 5 μM sodium orthovanadate inhibits dyneins (5, 41, 52). When these compounds were added to the motility chambers, they reduced the number of motile particles by 40% and 30%, respectively (Fig. 5A). The combination of both inhibitors together reduced the number of motile organelles by 50% (Fig. 5A).

More dramatic results were observed when the effects of these inhibitors on run length and velocity were examined. As can be seen in Fig. 5B, in the absence of inhibitors (buffer alone), plots of velocity against run length reveal two populations of motile particles: those with short run lengths (less than 20 μm) and highly variable velocities (from less than 0.5 μm/s to greater than 2 μm/s) and those with long run lengths (greater than 20 μm) and a nearly constant velocity of 1.0 to 1.4 μm/s. These more processive, constant velocity runs were completely abolished by AMP-PNP, whereas vanadate had a more modest effect but did reduce some of the shorter-distance motility. AMP-PNP sensitivity of the longer-distance runs is consistent with motility mediated by the highly processive motor kinesin. The less processive, vanadate-sensitive motor dynein appears to be responsible for some of the shorter-range runs but does not apparently play a major role in the motility events reconstituted in this in vitro system. These data are consistent with an assay system that faithfully reconstitutes the process of HSV egress.

Microtubule-bound HSV-associated organelles contain the *trans*-Golgi network marker TGN46. In our previous studies, we reported that the cytoplasmic organelles containing exocytosing HSV cofractionated with endosomal and TGN markers (30), but at that time, we could not distinguish between these populations. More recently, elegant studies by Turcotte and colleagues have demonstrated that the TGN is the principal site of HSV envelopment and egress (63). As a further test of

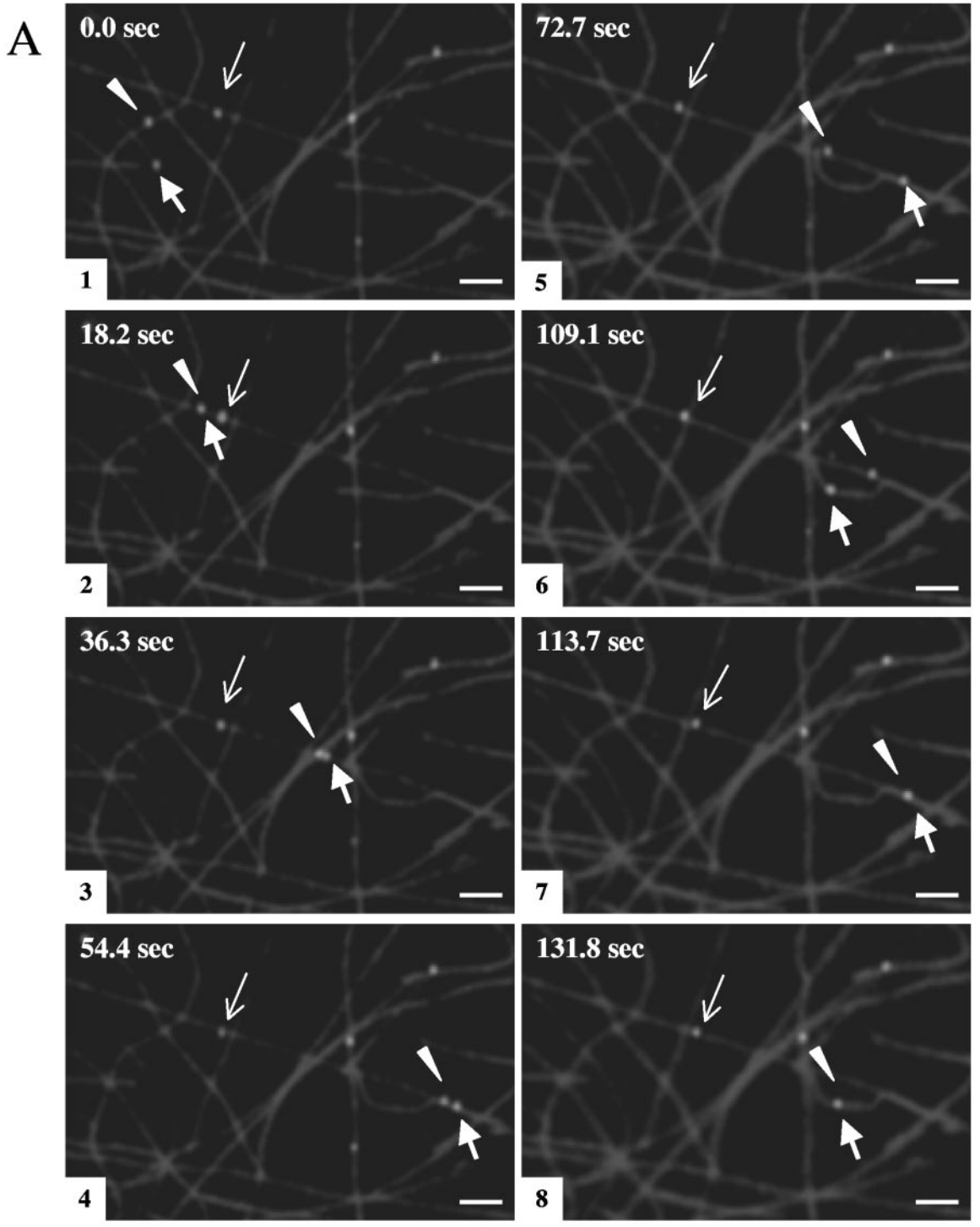

FIG. 2. Membrane-associated HSV capsids exhibit ATP-dependent movement along microtubules. Fluorescent HSV-bearing organelles were attached to rhodamine-labeled microtubules as described in the legend of Fig. 1. Following the addition of 500 μM ATP, sequential images were taken using time lapse video microscopy. Eight video frames are shown at selected intervals, as indicated in the upper left corner of each panel. (A) Two particles (thick arrow and arrowhead) move along the microtubules throughout the course of imaging, frequently moving from one microtubule to another at points of intersection, and they occasionally merge (frames 2 and 7) and split apart (frame 3). The average velocity of these particles is ~0.6 μm/s. A third particle (thin arrow) moves at a much slower rate (an average of ~0.02 μm/s). (B) One particle (arrow) translocates along microtubules, traveling a total distance of ~131 μm, switching between microtubules at microtubule junctions (indicated by * in frame 8) and ending its movement at the tip of the microtubule (frame 8). The other particle (arrowhead) stalls after moving ~22 μm (frame 5). Tracings of these HSV particle movements are shown in frame 8. Bar, 10 μm.

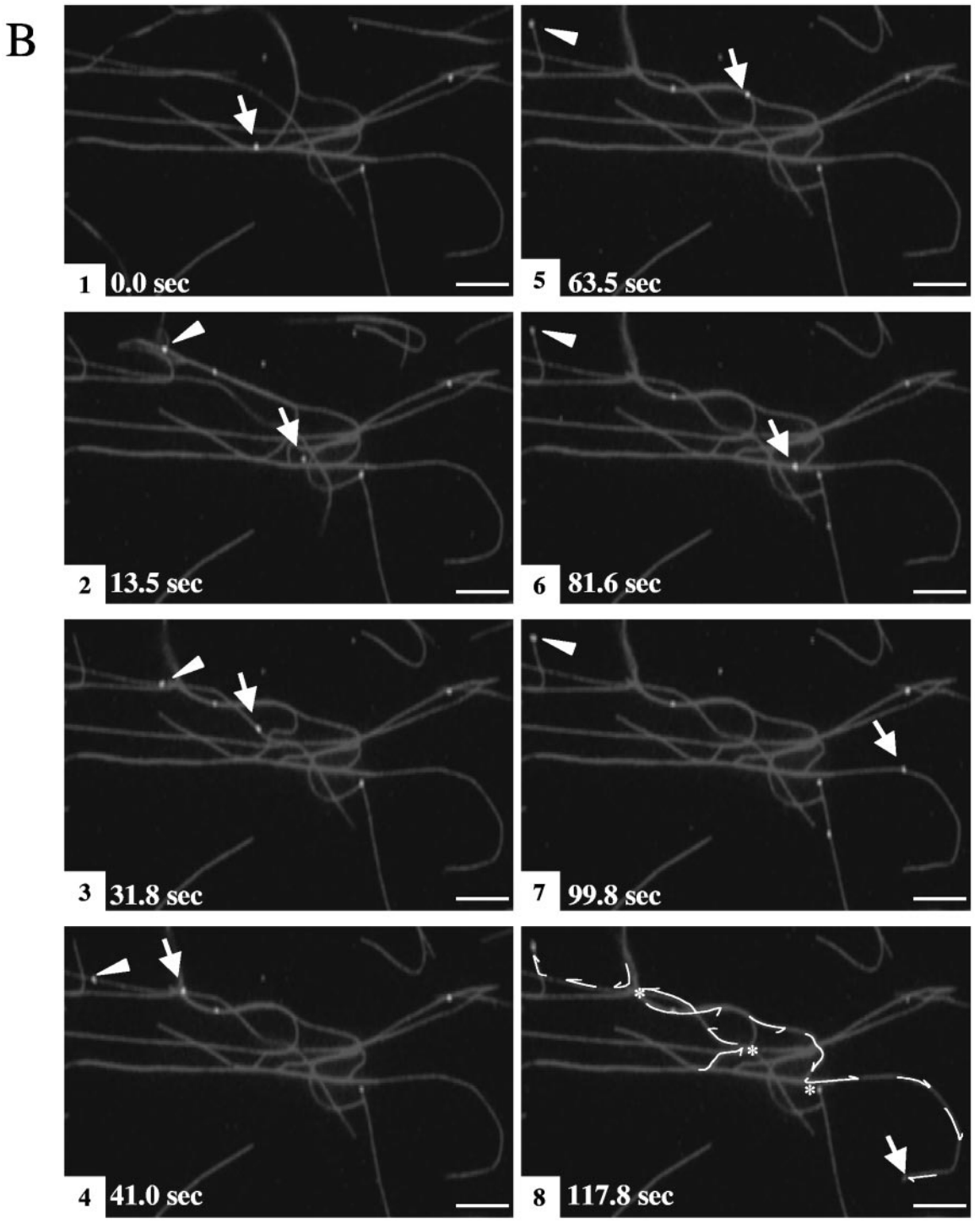

FIG. 2—*Continued.*

the validity of our in vitro assay system, we examined the origin of the microtubule-binding HSV-containing organelles using immunofluorescence microscopy. Microtubule-bound organelles were probed with antibodies against the early endosomal markers Rab4 and Rab5, the late endosomal marker Rab7, and the TGN marker TGN46. Representative fluorescence fields are shown in Fig. 6A, with HSV capsids in green, microtubules in red, and the organellar antigen in blue (colocalization of HSV with an organellar antigen generates a light blue color or white when the particle is directly over the red microtubule). We observed extensive colocalization of HSV with TGN46, but we saw little colocalization with the Rab markers. Quantitative analysis of these fields (Fig. 6B) indicated that ~58% of microtubule-bound virus-containing organelles were

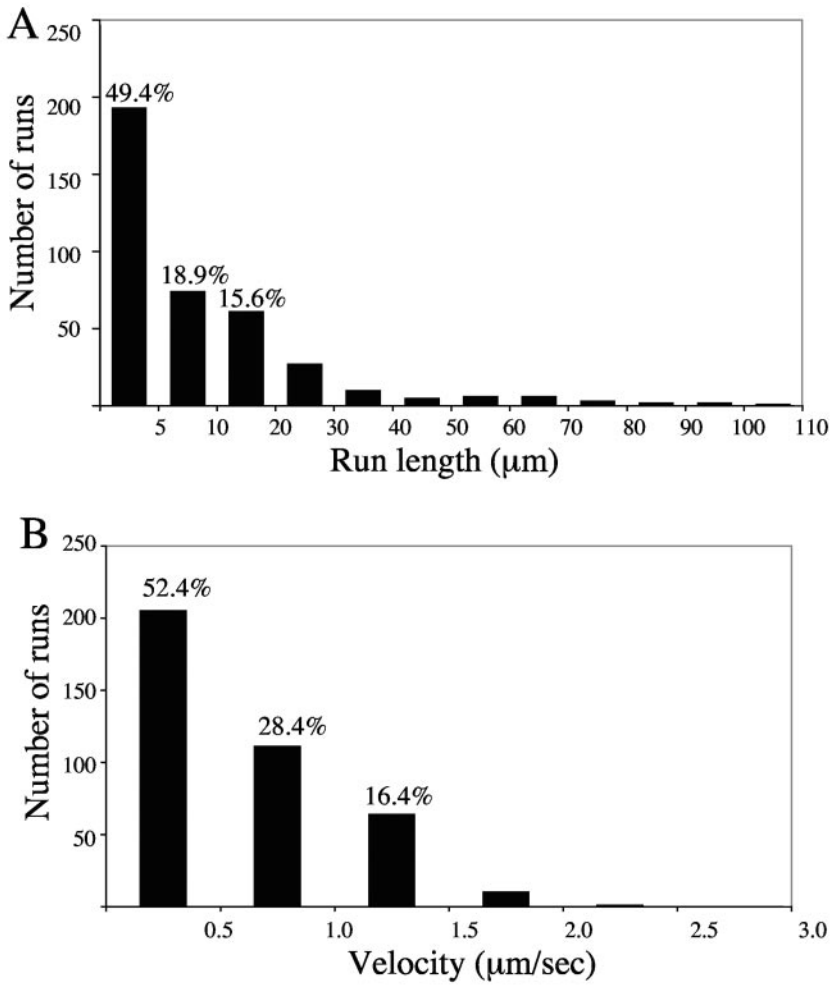

FIG. 3. Analysis of HSV particle movements. Microtubule motility events like those shown in Fig. 2 were quantitated for 391 green fluorescent particles. (A) Histogram of run lengths of motile HSV. The pixel lengths of each run were measured as described in Materials and Methods and converted to micrometers. The average run length was 11.81 ± 0.89 μm. The percentage of particles that traveled less than 5 μm, between 5 and 10 μm, and between 10 and 20 μm is indicated above the respective bars. (B) Histogram of velocity of motile HSV. The average velocity of each run was calculated by dividing the run length by its temporal duration. The overall average velocity was 0.58 ± 0.02 μm/s. The percentage of particles with velocities less than 0.5 μm/s, between 0.5 and 1.0 μm/s, and between 1.0 and 1.5 μm/s is indicated above the respective bars.

associated with TGN46, whereas less than 20% colocalized with each endosomal marker.

DISCUSSION

The purpose of this study was to develop an assay system to facilitate molecular analysis of microtubule-dependent HSV egress. To do this, we used the GFP-tagged HSV strain K26GFP (18), techniques we previously described for the isolation of cytoplasmic organelles containing HSV (30), and optical microchambers designed to monitor microtubule-based endosomal traffic in vitro (52). The HSV-associated structures prepared in these studies include fully enveloped capsids within organelles and capsids associated with the surface of organelles, as we previously reported (30). They are also strikingly similar in appearance to the HSV-associated organelles previously isolated by Satpute-Krishnan and colleagues in their study of anterograde HSV transport in the squid giant axon (56). Our immunocytochemical studies revealed that these membranous organelles also frequently contain the *trans*-Golgi network marker TGN46, also consistent with previous work (30, 48, 56). More recently, elegant studies by Turcotte and colleagues have demonstrated that the TGN is indeed the principal site of HSV envelopment and egress (63), as is also likely to be the case for varicella-zoster virus (1–3, 25, 29, 40, 65, 71, 72), PRV (10–12, 23, 24, 27), and human cytomegalovirus (15, 33, 35, 36). Nevertheless, our microtubule-bound organellar population is clearly heterogenous, and we cannot at the present time identify which HSV-associated organelles are motile.

We found that the isolated HSV-containing organellar structures were capable of efficiently binding to purified microtubules in vitro (approximately 62% of the fluorescent organelles bound). We could also reconstitute the transport of the HSV particles along microtubules upon the addition of ATP. On average, the motility efficiency was ~18%. At elevated ATP

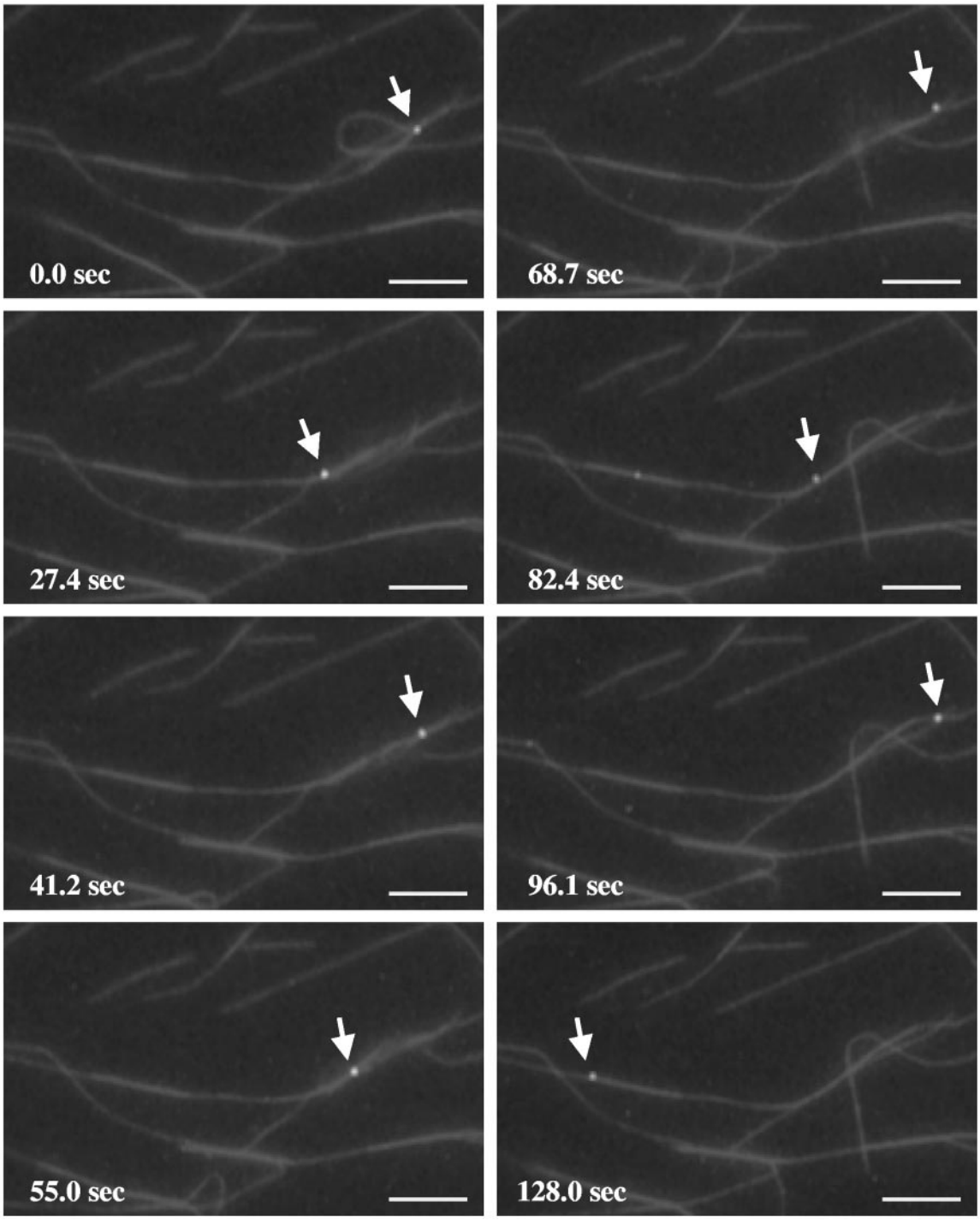

FIG. 4. HSV-associated particles move bidirectionally on the microtubules. Eight time lapse frames are shown. A particle (arrow) exhibits back-and-forth movement. Bar, 10 μm.

concentrations (~5 mM), the microtubules themselves glided and bent actively, demonstrating that some soluble motor proteins are also present in the preparation of cytoplasmic virus (data not shown). It has been unclear whether HSV egress in axons is as capsids, tegument and possibly membrane-bound capsids, enveloped mature particles inside organelles, or some combination of all three (8, 17, 19, 20, 32, 45, 49, 50, 54, 58). Ultrastructural analysis of our microtubule-bound preparation revealed that approximately 67% of the bound HSV particles were naked capsids, and the remainder were membrane-associated capsids or enveloped virions within organelles (data not shown). It remains unclear whether one or the other population or both are the motile particles that we observed.

The average run length (11.8 μm) in our in vitro system

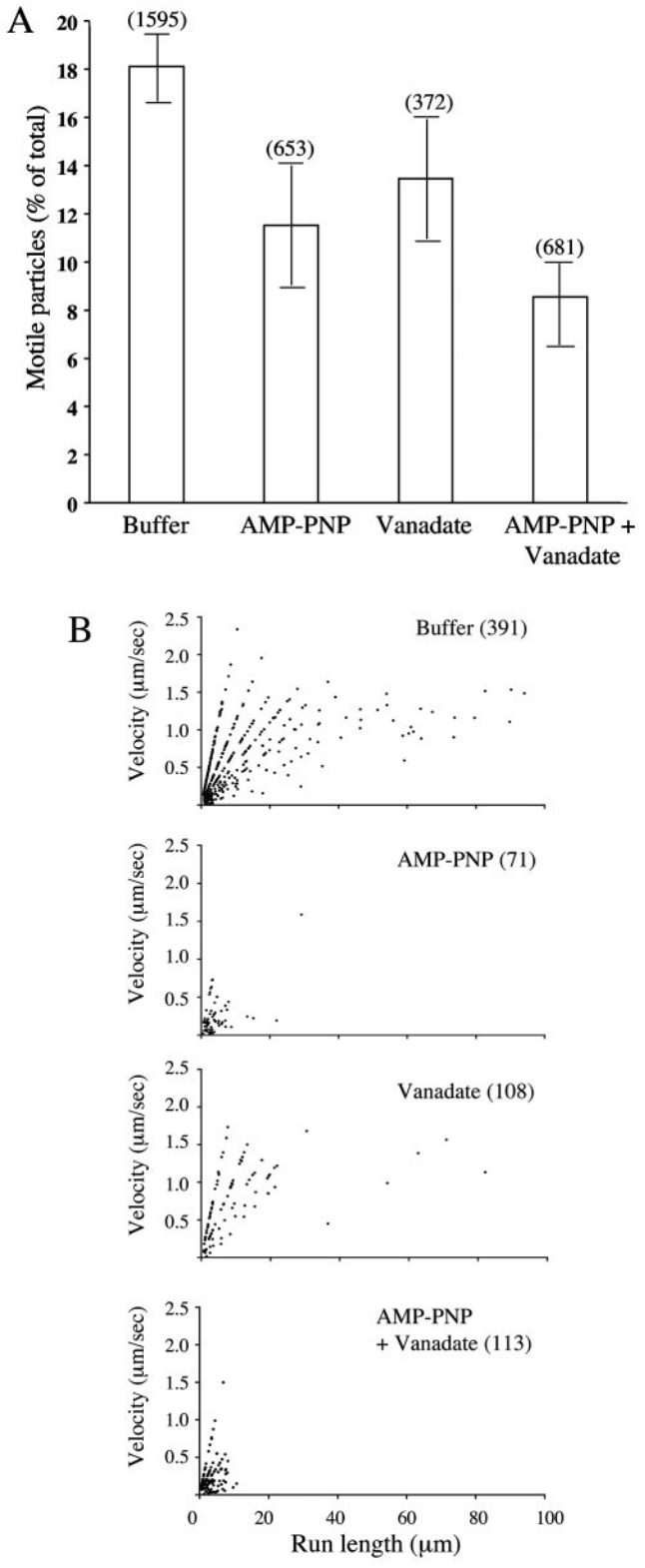

FIG. 5. Effects of microtubule motor inhibitors on HSV particle movement. Motility studies similar to those described in the legend of Fig. 3 were performed in the presence of AMP-PNP, sodium orthovanadate, or a mixture of the two or with buffer alone. (A) Effect of inhibitors on numbers of motile particles. The bars in the graph indicate the percentages of microtubule-bound HSV-associated particles that moved upon the addition of 500 μM ATP under each of the conditions tested. Error bars represent standard errors of the means. The number of microtubule-bound HSV particles examined in each experiment is shown in parentheses above each bar. (B) Effect of inhibitors upon the run length and velocity of particle motility. The number of runs examined under each of the four conditions is indicated in parentheses.

(Fig. 3A) is comparable to the 13.1-μm average seen for PRV in vivo using neuronal cell cultures (58). The average velocity (0.58 μm/s) of movement in our chamber system (Fig. 3B) is also in good agreement with the rate of anterograde HSV transport (0.56 to 0.83 μm/s) estimated in a dual cell culture chamber system (54) but slower than the average rate of anterograde transport of HSV (0.9 μm/s) in a squid axon system (56) or that of PRV (1.97 μm/s) in sensory neurons (58). The differences in rates may be a consequence of the minimal nature of our assay system. Unlike previous studies of anterograde trafficking using cytoplasmic HSV (56), our analysis is entirely in vitro, making use of microtubules polymerized from purified tubulin rather than studying trafficking in living axons (56, 58). Therefore, cellular factors that might contribute to increased motility may well be absent from this system. Alternatively, as discussed below, our average velocity calculation may be an underestimate of the true velocity of anterograde transport in our system.

We observed that some particles moved bidirectionally, indicating that they could be associated with plus-end and minus-end motors simultaneously (Fig. 4) or, alternatively, are simply switching to an adjacent antiparallel microtubule. Bidirectional motion is seen during transport of herpesvirus particles from the cell body along the axon to the nerve terminal (58). Several studies indicated that the minus-end motor dynein and the plus-end motor kinesin may be coordinated via a multimeric protein complex, dynactin, which is known to physically interact with both motors (16, 28, 47, 66) and which plays a role in retrograde transport of HSV capsids during entry (21). The need to regulate bidirectional movement is particularly acute at the TGN as a result of the substantial sorting and trafficking processes that occur there (31, 39, 43, 55, 61, 68).

To gain further insight into the molecular details of virus movement, we tested compounds that specifically inhibit motor activity. These inhibitors reduced but did not completely abolish the number of motility events (Fig. 5A), probably because motors were prebound with ATP and had to undergo at least one round of ATP hydrolysis, ADP release, and motion before associating with the inhibitory compound. The effect of inhibitors on the type of motion observed (Fig. 5B) was more informative. Normally, in the absence of inhibitors, particles either moved with short run lengths (less than 20 μm) and very variable velocities (from less than 0.5 μm/s to greater than 2 μm/s) or exhibited long run lengths (greater than 20 μm) and a nearly constant velocity of 1.0 to 1.4 μm/s. These more processive, constant-velocity runs were completely abolished by AMP-PNP, suggesting that they are kinesin mediated. These runs may therefore correspond to the anterograde trafficking of herpesvirus particles seen in axons, and their velocities are in good agreement with those observed in vivo (38, 42, 44, 54, 56, 58). AMP-PNP also inhibited some of the short-distance, low-velocity events, suggesting that some of these

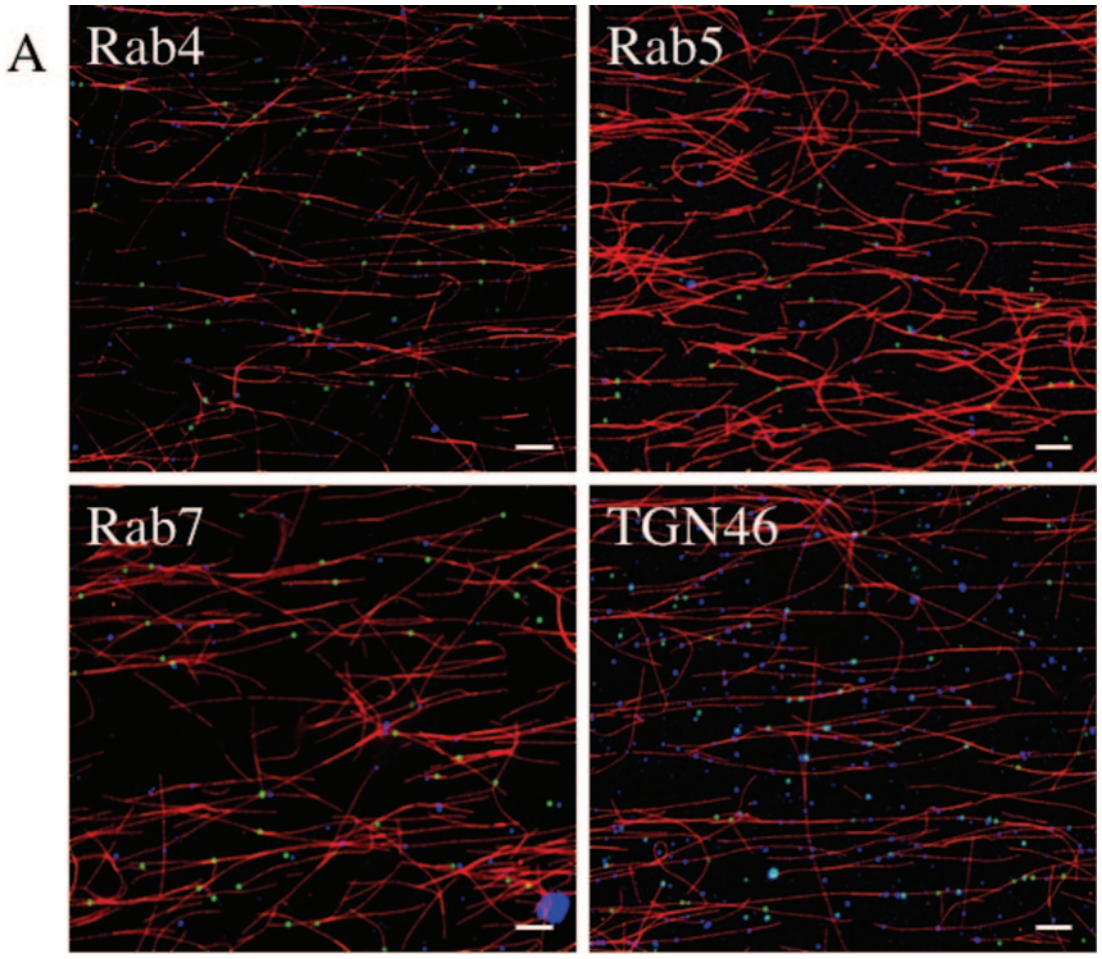

FIG. 6. Microtubule-bound HSV-associated particles are enriched for the *trans*-Golgi network marker TGN46. HSV K26GFP-associated cytoplasmic organelles were bound to rhodamine-labeled microtubules as shown in Fig. 1A and then incubated with antibodies against various organellar markers and a Cy5-labeled secondary antibody. (A) Representative fields resulting from such incubations, with the organellar antigen identified in the upper left corner of each panel and indicated by blue fluorescence. (B) Quantitative analysis of colocalization of HSV-associated particles with organellar markers. The bars in the graph represent the percentages of microtubule-bound HSV particles colocalizing with each of the organellar markers indicated in A. The error bars represent standard errors of the means.

events are also kinesin mediated. The much greater frequency and processivity of kinesin-mediated trafficking events over those that are vanadate sensitive (and thus dynein mediated) in our system (Fig. 5B) appear to also faithfully reproduce the situation in vivo, where movement to the axon terminal is saltatory and bidirectional, but anterograde motion is favored (45, 58). Although the data presented in Fig. 5B appear to fall along discrete lines, this is simply an artifact due to the constant sampling intervals used during imaging (see Materials and Methods).

This in vitro HSV egress assay is a minimal, simple system that is extremely biochemically accessible. It provides a model system where cellular or viral components necessary for virus motility can be identified by their ability to stimulate or modulate traffic.

ACKNOWLEDGMENTS

This work was supported by NIH program project grant DK41918 (to A.W.W.) and by R01 AI38265 (to D.W.W.).

HSV strain K26GFP was a kind gift from Prashant Desai. We thank Eustratios Bananis, Phyllis Novikoff, and Richard Stockert for helpful discussions.

REFERENCES

1. **Alconada, A., U. Bauer, L. Baudoux, J. Piette, and B. Hoflack.** 1998. Intracellular transport of the glycoproteins gE and gI of the varicella-zoster virus. gE accelerates the maturation of gI and determines its accumulation in the trans-Golgi network. J. Biol. Chem. **273:**13430–13436.
2. **Alconada, A., U. Bauer, and B. Hoflack.** 1996. A tyrosine-based motif and a casein kinase II phosphorylation site regulate the intracellular trafficking of the varicella-zoster virus glycoprotein I, a protein localized in the trans-Golgi network. EMBO J. **15:**6096–6110.
3. **Alconada, A., U. Bauer, B. Sodeik, and B. Hoflack.** 1999. Intracellular traffic of herpes simplex virus glycoprotein gE: characterization of the sorting signals required for its *trans*-Golgi network localization. J. Virol. **73:**377–387.
4. **Avitabile, E., S. Di Gaeta, M. R. Torrisi, P. L. Ward, B. Roizman, and G. Campadelli-Fiume.** 1995. Redistribution of microtubules and Golgi apparatus in herpes simplex virus-infected cells and their role in viral exocytosis. J. Virol. **69:**7472–7482.
5. **Bananis, E., S. Nath, K. Gordon, P. Satir, R. J. Stockert, J. W. Murray, and A. W. Wolkoff.** 2004. Microtubule-dependent movement of late endocytic vesicles in vitro: requirements for dynein and kinesin. Mol. Biol. Cell **15:** 3688–3697.
6. **Bearer, E. L., X. O. Breakefield, D. Schuback, T. S. Reese, and J. H. LaVail.** 2000. Retrograde axonal transport of herpes simplex virus: evidence for a single mechanism and a role for tegument. Proc. Natl. Acad. Sci. USA **97:**8146–8150.
7. **Beitia Ortiz de Zarate, I., K. Kaelin, and F. Rozenberg.** 2004. Effects of mutations in the cytoplasmic domain of herpes simplex virus type 1 glycoprotein B on intracellular transport and infectivity. J. Virol. **78:**1540–1551.
8. **Benboudjema, L., M. Mulvey, Y. Gao, S. W. Pimplikar, and I. Mohr.** 2003. Association of the herpes simplex virus type 1 Us11 gene product with the cellular kinesin light-chain-related protein PAT1 results in the redistribution of both polypeptides. J. Virol. **77:**9192–9203.
9. **Brack, A. R., B. G. Klupp, H. Granzow, R. Tirabassi, L. W. Enquist, and T. C. Mettenleiter.** 2000. Role of the cytoplasmic tail of pseudorabies virus glycoprotein E in virion formation. J. Virol. **74:**4004–4016.
10. **Brideau, A. D., J. P. Card, and L. W. Enquist.** 2000. Role of pseudorabies virus Us9, a type II membrane protein, in infection of tissue culture cells and the rat nervous system. J. Virol. **74:**834–845.
11. **Brideau, A. D., T. del Rio, E. J. Wolffe, and L. W. Enquist.** 1999. Intracellular trafficking and localization of the pseudorabies virus Us9 type II envelope protein to host and viral membranes. J. Virol. **73:**4372–4384.
12. **Brideau, A. D., M. G. Eldridge, and L. W. Enquist.** 2000. Directional transneuronal infection by pseudorabies virus is dependent on an acidic internalization motif in the US9 cytoplasmic tail. J. Virol. **74:**4549–4561.
13. **Browne, H., S. Bell, T. Minson, and D. W. Wilson.** 1996. An endoplasmic reticulum-retained herpes simplex virus glycoprotein H is absent from secreted virions: evidence for reenvelopment during egress. J. Virol. **70:**4311–4316.
14. **Church, G. A., and D. W. Wilson.** 1997. Study of herpes simplex virus maturation during a synchronous wave of assembly. J. Virol. **71:**3603–3612.
15. **Crump, C. M., C. H. Hung, L. Thomas, L. Wan, and G. Thomas.** 2003. Role of PACS-1 in trafficking of human cytomegalovirus glycoprotein B and virus production. J. Virol. **77:**11105–11113.
16. **Deacon, S. W., A. S. Serpinskaya, P. S. Vaughan, M. Lopez Fanarraga, I. Vernos, K. T. Vaughan, and V. I. Gelfand.** 2003. Dynactin is required for bidirectional organelle transport. J. Cell Biol. **160:**297–301.
17. **Del Rio, T., T. H. Ch'ng, E. A. Flood, S. P. Gross, and L. W. Enquist.** 2005. Heterogeneity of a fluorescent tegument component in single pseudorabies virus virions and enveloped axonal assemblies. J. Virol. **79:**3903–3919.
18. **Desai, P., and S. Person.** 1998. Incorporation of the green fluorescent protein into the herpes simplex virus type 1 capsid. J. Virol. **72:**7563–7568.
19. **Desai, P. J.** 2000. A null mutation in the UL36 gene of herpes simplex virus type 1 results in accumulation of unenveloped DNA-filled capsids in the cytoplasm of infected cells. J. Virol. **74:**11608–11618.
20. **Diefenbach, R. J., M. Miranda-Saksena, E. Diefenbach, D. J. Holland, R. A. Boadle, P. J. Armati, and A. L. Cunningham.** 2002. Herpes simplex virus tegument protein US11 interacts with conventional kinesin heavy chain. J. Virol. **76:**3282–3291.
21. **Dohner, K., A. Wolfstein, U. Prank, C. Echeverri, D. Dujardin, R. Vallee, and B. Sodeik.** 2002. Function of dynein and dynactin in herpes simplex virus capsid transport. Mol. Biol. Cell **13:**2795–2809.
22. **Douglas, M. W., R. J. Diefenbach, F. L. Homa, M. Miranda-Saksena, F. J. Rixon, V. Vittone, K. Byth, and A. L. Cunningham.** 2004. Herpes simplex virus type 1 capsid protein VP26 interacts with dynein light chains RP3 and Tctex1 and plays a role in retrograde cellular transport. J. Biol. Chem. **279:**28522–28530.
23. **Fuchs, W., H. Granzow, and T. C. Mettenleiter.** 1997. Functional complementation of UL3.5-negative pseudorabies virus by the bovine herpesvirus 1 UL3.5 homolog. J. Virol. **71:**8886–8892.
24. **Fuchs, W., B. G. Klupp, H. Granzow, H. J. Rziha, and T. C. Mettenleiter.** 1996. Identification and characterization of the pseudorabies virus UL3.5 protein, which is involved in virus egress. J. Virol. **70:**3517–3527.
25. **Gershon, A. A., D. L. Sherman, Z. Zhu, C. A. Gabel, R. T. Ambron, and M. D. Gershon.** 1994. Intracellular transport of newly synthesized varicella-zoster virus: final envelopment in the *trans*-Golgi network. J. Virol. **68:**6372–6390.
26. **Granzow, H., B. G. Klupp, W. Fuchs, J. Veits, N. Osterrieder, and T. C. Mettenleiter.** 2001. Egress of alphaherpesviruses: comparative ultrastructural study. J. Virol. **75:**3675–3684.
27. **Granzow, H., F. Weiland, A. Jons, B. G. Klupp, A. Karger, and T. C. Mettenleiter.** 1997. Ultrastructural analysis of the replication cycle of pseudorabies virus in cell culture: a reassessment. J. Virol. **71:**2072–2082.
28. **Gross, S. P., M. A. Welte, S. M. Block, and E. F. Wieschaus.** 2002. Coordination of opposite-polarity microtubule motors. J. Cell Biol. **156:**715–724.
29. **Hambleton, S., M. D. Gershon, and A. A. Gershon.** 2004. The role of the trans-Golgi network in varicella zoster virus biology. Cell. Mol. Life Sci. **61:**3047–3056.
30. **Harley, C. A., A. Dasgupta, and D. W. Wilson.** 2001. Characterization of herpes simplex virus-containing organelles by subcellular fractionation: role for organelle acidification in assembly of infectious particles. J. Virol. **75:** 1236–1251.
31. **Hirokawa, N.** 1998. Kinesin and dynein superfamily proteins and the mechanism of organelle transport. Science **279:**519–526.
32. **Holland, D. J., M. Miranda-Saksena, R. A. Boadle, P. Armati, and A. L. Cunningham.** 1999. Anterograde transport of herpes simplex virus proteins in axons of peripheral human fetal neurons: an immunoelectron microscopy study. J. Virol. **73:**8503–8511.
33. **Homman-Loudiyi, M., K. Hultenby, W. Britt, and C. Söderberg-Nauclér.** 2003. Envelopment of human cytomegalovirus occurs by budding into Golgi-derived vacuole compartments positive for gB, Rab 3, trans-Golgi network 46, and mannosidase II. J. Virol. **77:**3191–3203.
34. **Howard, J., and A. A. Hyman.** 1993. Preparation of marked microtubules for the assay of the polarity of microtubule-based motors by fluorescence microscopy. Methods Cell Biol. **39:**105–113.
35. **Jarvis, M. A., K. N. Fish, C. Soderberg-Naucler, D. N. Streblow, H. L. Meyers, G. Thomas, and J. A. Nelson.** 2002. Retrieval of human cytomegalovirus glycoprotein B from cell surface is not required for virus envelopment in astrocytoma cells. J. Virol. **76:**5147–5155.
36. **Jarvis, M. A., T. R. Jones, D. D. Drummond, P. P. Smith, W. J. Britt, J. A. Nelson, and C. J. Baldick.** 2004. Phosphorylation of human cytomegalovirus glycoprotein B (gB) at the acidic cluster casein kinase 2 site (Ser_{900}) is required for localization of gB to the *trans*-Golgi network and efficient virus replication. J. Virol. **78:**285–293.
37. **Johnson, D. C., M. Webb, T. W. Wisner, and C. Brunetti.** 2001. Herpes simplex virus gE/gI sorts nascent virions to epithelial cell junctions, promoting virus spread. J. Virol. **75:**821–833.
38. **Johnson, K. A., and S. P. Gilbert.** 1995. Pathway of the microtubule-kinesin ATPase. Biophys. J. **68:**173S–176S.
39. **Kamal, A., and L. S. Goldstein.** 2002. Principles of cargo attachment to cytoplasmic motor proteins. Curr. Opin. Cell Biol. **14:**63–68.
40. **Kenyon, T. K., J. I. Cohen, and C. Grose.** 2002. Phosphorylation by the varicella-zoster virus ORF47 protein serine kinase determines whether endocytosed viral gE traffics to the *trans*-Golgi network or recycles to the cell membrane. J. Virol. **76:**10980–10993.
41. **Kobayashi, T., T. Martensen, J. Nath, and M. Flavin.** 1978. Inhibition of dynein ATPase by vanadate, and its possible use as a probe for the role of dynein in cytoplasmic motility. Biochem. Biophys. Res. Commun. **81:**1313–1318.
42. **Kristensson, K., E. Lycke, M. Roytta, B. Svennerholm, and A. Vahlne.** 1986. Neuritic transport of herpes simplex virus in rat sensory neurons in vitro. Effects of substances interacting with microtubular function and axonal flow [nocodazole, taxol and erythro-9-3-(2-hydroxynonyl)adenine]. J. Gen. Virol. **67:**2023–2028.
43. **Lane, J., and V. Allan.** 1998. Microtubule-based membrane movement. Biochim. Biophys. Acta **1376:**27–55.
44. **LaVail, J. H., K. S. Topp, P. A. Giblin, and J. A. Garner.** 1997. Factors that contribute to the transneuronal spread of herpes simplex virus. J. Neurosci. Res. **49:**485–496.
45. **Luxton, G. W., S. Haverlock, K. E. Coller, S. E. Antinone, A. Pincetic, and G. A. Smith.** 2005. Targeting of herpesvirus capsid transport in axons is coupled to association with specific sets of tegument proteins. Proc. Natl. Acad. Sci. USA **102:**5832–5837.
46. **Lycke, E., K. Kristensson, B. Svennerholm, A. Vahlne, and R. Ziegler.** 1984. Uptake and transport of herpes simplex virus in neurites of rat dorsal root ganglia cells in culture. J. Gen. Virol. **65:**55–64.
47. **Martin, M., S. J. Iyadurai, A. Gassman, J. G. Gindhart, Jr., T. S. Hays, and W. M. Saxton.** 1999. Cytoplasmic dynein, the dynactin complex, and kinesin are interdependent and essential for fast axonal transport. Mol. Biol. Cell **10:**3717–3728.
48. **McMillan, T. N., and D. C. Johnson.** 2001. Cytoplasmic domain of herpes simplex virus gE causes accumulation in the *trans*-Golgi network, a site of virus envelopment and sorting of virions to cell junctions. J. Virol. **75:**1928–1940.
49. **Miranda-Saksena, M., P. Armati, R. A. Boadle, D. J. Holland, and A. L.**

Cunningham. 2000. Anterograde transport of herpes simplex virus type 1 in cultured, dissociated human and rat dorsal root ganglion neurons. J. Virol. **74:**1827–1839.
50. **Miranda-Saksena, M., R. A. Boadle, P. Armati, and A. L. Cunningham.** 2002. In rat dorsal root ganglion neurons, herpes simplex virus type 1 tegument forms in the cytoplasm of the cell body. J. Virol. **76:**9934–9951.
51. **Murray, J. W., E. Bananis, and A. W. Wolkoff.** 2002. Immunofluorescence microchamber technique for characterizing isolated organelles. Anal. Biochem. **305:**55–67.
52. **Murray, J. W., E. Bananis, and A. W. Wolkoff.** 2000. Reconstitution of ATP-dependent movement of endocytic vesicles along microtubules in vitro: an oscillatory bidirectional process. Mol. Biol. Cell **11:**419–433.
53. **Norrild, B., V. P. Lehto, and I. Virtanen.** 1986. Organization of cytoskeleton elements during herpes simplex virus type 1 infection of human fibroblasts: an immunofluorescence study. J. Gen. Virol. **67:**97–105.
54. **Penfold, M. E., P. Armati, and A. L. Cunningham.** 1994. Axonal transport of herpes simplex virions to epidermal cells: evidence for a specialized mode of virus transport and assembly. Proc. Natl. Acad. Sci. USA **91:**6529–6533.
55. **Polishchuk, E. V., A. Di Pentima, A. Luini, and R. S. Polishchuk.** 2003. Mechanism of constitutive export from the Golgi: bulk flow via the formation, protrusion, and en bloc cleavage of large trans-Golgi network tubular domains. Mol. Biol. Cell **14:**4470–4485.
56. **Satpute-Krishnan, P., J. A. DeGiorgis, and E. L. Bearer.** 2003. Fast anterograde transport of herpes simplex virus: role for the amyloid precursor protein of Alzheimer's disease. Aging Cell **2:**305–318.
57. **Skepper, J. N., A. Whiteley, H. Browne, and A. Minson.** 2001. Herpes simplex virus nucleocapsids mature to progeny virions by an envelopment→deenvelopment→reenvelopment pathway. J. Virol. **75:**5697–5702.
58. **Smith, G. A., S. P. Gross, and L. W. Enquist.** 2001. Herpesviruses use bidirectional fast-axonal transport to spread in sensory neurons. Proc. Natl. Acad. Sci. USA **98:**3466–3470.
59. **Smith, G. A., L. Pomeranz, S. P. Gross, and L. W. Enquist.** 2004. Local modulation of plus-end transport targets herpesvirus entry and egress in sensory axons. Proc. Natl. Acad. Sci. USA **101:**16034–16039.
60. **Sodeik, B., M. W. Ebersold, and A. Helenius.** 1997. Microtubule-mediated transport of incoming herpes simplex virus 1 capsids to the nucleus. J. Cell Biol. **136:**1007–1021.
61. **Toomre, D., P. Keller, J. White, J. C. Olivo, and K. Simons.** 1999. Dual-color visualization of trans-Golgi network to plasma membrane traffic along microtubules in living cells. J. Cell Sci. **112:**21–33.
62. **Topp, K. S., L. B. Meade, and J. H. LaVail.** 1994. Microtubule polarity in the peripheral processes of trigeminal ganglion cells: relevance for the retrograde transport of herpes simplex virus. J. Neurosci. **14:**318–325.
63. **Turcotte, S., J. Letellier, and R. Lippé.** 2005. Herpes simplex virus type 1 capsids transit by the *trans*-Golgi network, where viral glycoproteins accumulate independently of capsid egress. J. Virol. **79:**8847–8860.
64. **Vale, R. D., F. Malik, and D. Brown.** 1992. Directional instability of microtubule transport in the presence of kinesin and dynein, two opposite polarity motor proteins. J. Cell Biol. **119:**1589–1596.
65. **Wang, Z.-H., M. D. Gershon, O. Lungu, Z. Zhu, S. Mallory, A. M. Arvin, and A. A. Gershon.** 2001. Essential role played by the C-terminal domain of glycoprotein I in envelopment of varicella-zoster virus in the *trans*-Golgi network: interactions of glycoproteins with tegument. J. Virol. **75:**323–340.
66. **Waterman-Storer, C. M., S. B. Karki, S. A. Kuznetsov, J. S. Tabb, D. G. Weiss, G. M. Langford, and E. L. Holzbaur.** 1997. The interaction between cytoplasmic dynein and dynactin is required for fast axonal transport. Proc. Natl. Acad. Sci. USA **94:**12180–12185.
67. **Whiteley, A., B. Bruun, T. Minson, and H. Browne.** 1999. Effects of targeting herpes simplex virus type 1 gD to the endoplasmic reticulum and *trans*-Golgi network. J. Virol. **73:**9515–9520.
68. **Wisner, T. W., and D. C. Johnson.** 2004. Redistribution of cellular and herpes simplex virus proteins from the trans-Golgi network to cell junctions without enveloped capsids. J. Virol. **78:**11519–11535.
69. **Yamamoto, T., S. Otani, and H. Shiraki.** 1973. Ultrastructure of herpes simplex virus infection of the nervous system of mice. Acta Neuropathol. **26:**285–299.
70. **Ye, G. J., K. T. Vaughan, R. B. Vallee, and B. Roizman.** 2000. The herpes simplex virus 1 UL34 protein interacts with a cytoplasmic dynein intermediate chain and targets nuclear membrane. J. Virol. **74:**1355–1363.
71. **Zhu, Z., M. D. Gershon, Y. Hao, R. T. Ambron, C. A. Gabel, and A. A. Gershon.** 1995. Envelopment of varicella-zoster virus: targeting of viral glycoproteins to the *trans*-Golgi network. J. Virol. **69:**7951–7959.
72. **Zhu, Z., Y. Hao, M. D. Gershon, R. T. Ambron, and A. A. Gershon.** 1996. Targeting of glycoprotein I (gE) of varicella-zoster virus to the *trans*-Golgi network by an AYRV sequence and an acidic amino acid-rich patch in the cytosolic domain of the molecule. J. Virol. **70:**6563–6575.